Investigation of Gellan Networks and Gels by Atomic Force Microscopy

A. P. Gunning, A. R. Kirby, M. J. Ridout, G. J. Brownsey, and V. J. Morris*

Institute of Food Research, Norwich Laboratory, Norwich Research Park, Colney, Norwich NR4 7UA, U.K.

Received May 14, 1996; Revised Manuscript Received July 24, 1996[⊗]

ABSTRACT: Methods previously developed for the atomic force microscopy (AFM) imaging of individual polysaccharides (Kirby, A. R.; Gunning, A. P.; Morris, V. J. *Biopolymers* **1996**, *38*, 355−366) have been extended in order to image networks and gels formed by the bacterial polysaccharide gellan gum. Networks were formed by air-drying solutions of K^+ gellan onto freshly cleaved mica. AFM images were obtained in the direct current contact mode at constant force under butanol. Network formation can be inhibited by diluting the stock gellan solution or by converting K^+ gellan into the tetramethylammonium salt form. Inhibition of network formation led to AFM images of heterogeneous populations of gellan aggregates (gel precursors). Attempts have been made to image the surface of bulk aqueous gellan gels under butanol. The quality of the images obtained improved with increasing gel modulus. For rigid acid-set gellan gels, molecular resolution was achieved, revealing a bifurcated branched fibrous network.

Introduction

Atomic force microscopy (AFM) is a new and powerful method for studying biopolymers.[1−4] Recently methods have been developed for imaging polysaccharides,[4−8] in which polysaccharide solutions are deposited onto freshly cleaved mica and allowed to dry in air. This is a relatively mild preparative treatment and the molecules may even reside within a thin film of water on the mica surface.[9] Attempts to image polysaccharides in air by direct current (dc) contact mode AFM are very difficult, because any moisture that has condensed on the probe and the mica surface coalesces when they are brought close together. These "capillary forces" effectively "glue" the probe to the surface and, upon scanning, give rise to large shear forces which disrupt or displace the molecules.[2] This capillary force can be eliminated by reducing the relative humidity, although this approach is seldom used in practice. Recently alternating current (ac) mode imaging, which virtually eliminates the shear forces during scanning, has been shown to be a successful method for imaging biopolymers[8,10−13] including polysaccharides[8,13] in air without the need to control relative humidity. Most of these studies[10−13] report the use of ac tapping mode operation. Studies on scleroglucan[8] are said to have been made using true ac noncontact mode imaging, but the quality of the images presented suggests that the instrument may have actually been operating in the tapping mode. An alternative approach is to use conventional dc contact mode imaging under liquid.[4−7] For polysaccharides, water cannot be used because they are water soluble. However, imaging under precipitants such as butanol or propanol allows the capillary force to be eliminated and the imaging force controlled in order to optimize imaging conditions.[7] Under such conditions, AFM can be used to reveal the helical secondary structure of polysaccharides.[6] An alternative application is to probe polysaccharide association in areas such as polysaccharide gelation. Most models for polysaccharide gelation are based on physical−chemical studies and have concentrated on the detailed molecular structure of the junction zones within the gel. AFM offers a method for investigating such models for gelation and also for visualizing the long range distributions of macromolecules within the gel network. At present there are few AFM studies of networks and gels[4,7,14−17] and none of polysaccharide gels. This article describes attempts to visualize networks and gels formed by the bacterial polysaccharide gellan gum.

Experimental Section

Samples of deesterified gellan gum (Gelrite) were purchased from Kelco-AIL. Gelrite is predominantly in the potassium salt form. The tetramethylammonium (TMA) salt form of gellan was prepared in the following way. An aqueous 0.2% gellan solution was prepared by dissolving powdered Gelrite in distilled water contained within a sealed tube and heated to 95−100 °C. The sample was cooled to room temperature and the gellan precipitated at acid pH using 0.1 M HCl. The precipitate was collected by filtration, washed with successive rinses of water and ethanol, and redispersed in water. The polymer was dissolved by titration of an appropriate amount of 0.1 M tetramethylammonium hydroxide to return the pH of the sol to neutral (pH 7). This whole procedure was repeated twice in order to ensure complete conversion to the required salt form. The sample was stored as a freeze-dried powder.

The polysaccharide samples were dispersed in water to a concentration of ≈1 mg mL^{-1}, heated to ≈98 °C for 1−2 h while being stirred, and then cooled to room temperature. Samples for study by AFM were prepared in the following manner. The stock (1 mg mL^{-1}) sol was diluted to various concentrations in the range 1−10 μg mL^{-1}. Drops (2 μL) of the samples were deposited onto freshly cleaved mica surfaces and then allowed to dry in air (≈10 min). The samples were then imaged under butanol with no further treatment. Bulk 3D gels, thermally set, were prepared on mica by pipetting hot gellan sols onto the surface and allowing the samples to cool to room temperature. Gel samples were also imaged under butanol. Further details relating to the composition of 3D gels will be described later in this article.

The AFM used in this study was designed and manufactured by East Coast Scientific (Cambridge, UK). Its design and operation is described in the PhD thesis of Wong.[18] Direct current contact (repulsive force) imaging was carried out under constant force conditions (typically in the range 2−3 nN). Short narrow Nanoprobe cantilevers (Digital Instruments, Santa Barbara, CA) were used with a quoted force constant of 0.38 Nm^{-1}.

* Author for correspondence.

[⊗] Abstract published in *Advance ACS Abstracts,* September 15, 1996.

S0024-9297(96)00700-0 CCC: $12.00

Rheological studies were made using an Instron 3250 mechanical spectrometer in parallel plate geometry (platen diameter, 40 mm). Gels were prepared in plastic Petri dishes. The gels were removed from the Petri dishes for examination. The platens were coated with fine Emery paper to ensure good surface contact with the gels and to prevent slippage due to syneresis from the gels. The TMA gellan samples were tested in the Petri dishes. The dishes were stuck to the lower platen of the instrument.

Results and Discussion

Initial attempts to image gel networks were made using the microbial polysaccharide gellan gum. Gellan gum is an anionic heteropolysaccharide with a chemical structure[19−20] based on a regular tetrasaccharide repeat unit →3)-βDGlc-(1 → 4)-βDGlcA-(1 → 4)-βDGlc-(1 → 4)-αLRha(1→. The native form of gellan is esterified,[21] but the commercial product, Gelrite, used in the present studies is a completely deesterified form. The nature of the isolation and deesterification process results in a material predominantly in the K^+ salt form.[22−23]

Figure 1a,b shows AFM images of gellan networks formed after deposition of 10 μg mL^{-1} gellan sols onto freshly cleaved mica. After air-drying and imaging under butanol the AFM images reveal continuous branched fibrous networks. Although the images appear to be of a network comprising one large branched fibrous structure, higher resolution images (Figure 1b) reveal some polymer ends corresponding to the ends of short branches. Much as individual polysaccharides air-dried onto mica should retain water of hydration, it is to be expected that thin films, or essentially 2D networks, would be even more likely to retain some degree of hydration. Imaging under butanol may enhance dehydration, but it is believed that the images shown in Figure 1a,b demonstrate that AFM can be used to image polysaccharide networks.

The regular chemical structure of gellan makes it a simple model system for studying polysaccharide gelation, and recent papers[24,25] provide a description of current views on the mechanisms of gelation. Physical chemical methods have been used to model the details of the gelation process.[24−27] Gellan gum yields excellent X-ray diffraction patterns from oriented fibers prepared from gellan films.[28−34] Modeling of this data has produced atomic resolution helical structures of gellan[30−34] and atomic resolution models for the packing of these helices within the crystalline regions obtained in the presence of certain cations.[31−34] Thus, junction zones within gels are generally considered to consist of locally aggregated or crystalline arrays of gellan helices bound together by gel-promoting cations. Gelation is considered to involve two separable steps.[24,25] Gellan gels are thermoreversible.[24,25] Cooling is believed to involve gellan molecules undergoing a conformational change from the disordered "coil" form to the ordered helical structure. At sufficiently high concentration, adoption of the ordered form is accompanied by intermolecular association or aggregation. At this stage, the order−disorder transition is thermoreversible and shows no hysteresis. At concentrations above the critical concentration for gelation a weak network may be formed, but the "weak gel" structure breaks down under strain. Such effects are observed for the tetramethylammonium (TMA) salt form of gellan.[24,25] In the presence of gel-promoting cations, the gel networks formed at sufficiently high polymer concentration become permanent due to cation binding stabilizing the interhelical associations. At this point the gellan gels show thermal hysteresis. Different models for gellan gelation[24,25] invoke different types of association prior to cation binding and thus differ in their views on the large scale molecular structure of the gel.

Gelation of gellan gum is thermoreversible.[24,25] Why should a gel network form on air-drying gellan sols onto mica surfaces? At the stock gellan concentrations employed in the present study ($\leq$10 μg mL^{-1}) the polymer concentration will be too low to permit gelation. In pure water the polymer concentration will determine the ionic strength, and this in turn will determine the "helix−coil" transition temperature (T_c) and whether T_c lies above or below room temperature. If T_c is above room temperature, then the stock sols will actually be a dispersion of gellan aggregates or gel precursors. If, as seems likely at the high dilutions used in this study, T_c is below room temperature, then gellan will exist in the disordered "coil" form and will associate during air-drying as the increasing concentration raises the ionic strength and hence T_c. In both scenarios, when the polymer concentration exceeds the critical threshold concentration for gelation, the polymer can assemble into a gel network. In the presence of gel-promoting cations, a permanent gel network should be formed, but if gel-promoting cations are replaced by bulky TMA cations, then ion binding does not occur. However, on air-drying and hence concentration of the TMA ions, the conformational changes still occur, leading to aggregation. At low polymer concentrations gel precursors would be formed whereas at higher concentrations a weak gel structure should be formed.

Figure 2a,b compares the rheological behavior of K^+ gellan (Gelrite) and TMA^+ gellan samples. At a polymer concentration of 1.2% gellan the K^+ gellan sample forms a permanent gel network. G' (the storage modulus) is substantially greater than G'' (the loss modulus), and both are almost independent of frequency. The modulus is strain independent up to about 10% strain. By contrast TMA gellan at 1.2% concentration shows behavior characteristic of a fluid: $G'' > G'$ and both increase with frequency.

Figure 1c,d shows the effect of replacing K^+ by TMA^+ on the networks formed by air-drying gellan onto mica. The images obtained show a dispersion of complex branched fibrous structures. The images are unlike those shown in Figure 1a,b. In the present case, many polymer ends are visible in the images. The complex shape and size suggests that the majority of the branched structures are aggregates rather than individual gellan molecules. This is based on light scattering studies of gellan[35] which suggest linear molecules of average contour length $L_w = 611$ nm. Therefore, the branched structures are considered to be aggregates rather than individual molecules. Figure 1c,d shows an advantage of the use of a microscopic technique such as AFM. The complex heterogeneous ensemble of branched aggregates (gel precursors) would be difficult to characterize by most conventional biophysical methods which yield average properties of the system. The high contrast obtained in the AFM images makes them amenable to further analysis.

Another method for inhibiting gelation would be to reduce the bulk polymer concentration. At polymer concentrations $\leq$3 μg mL^{-1} continuous "gel" networks are not obtained after air-drying gellan solutions onto mica surfaces. This is illustrated in Figure 1e,f. Once again the AFM images reveal a complex heterogeneous population of branched fibrous aggregates.

The data presented provides information on gel precursors and gel networks. However, the method of network formation is somewhat contrived. Are such

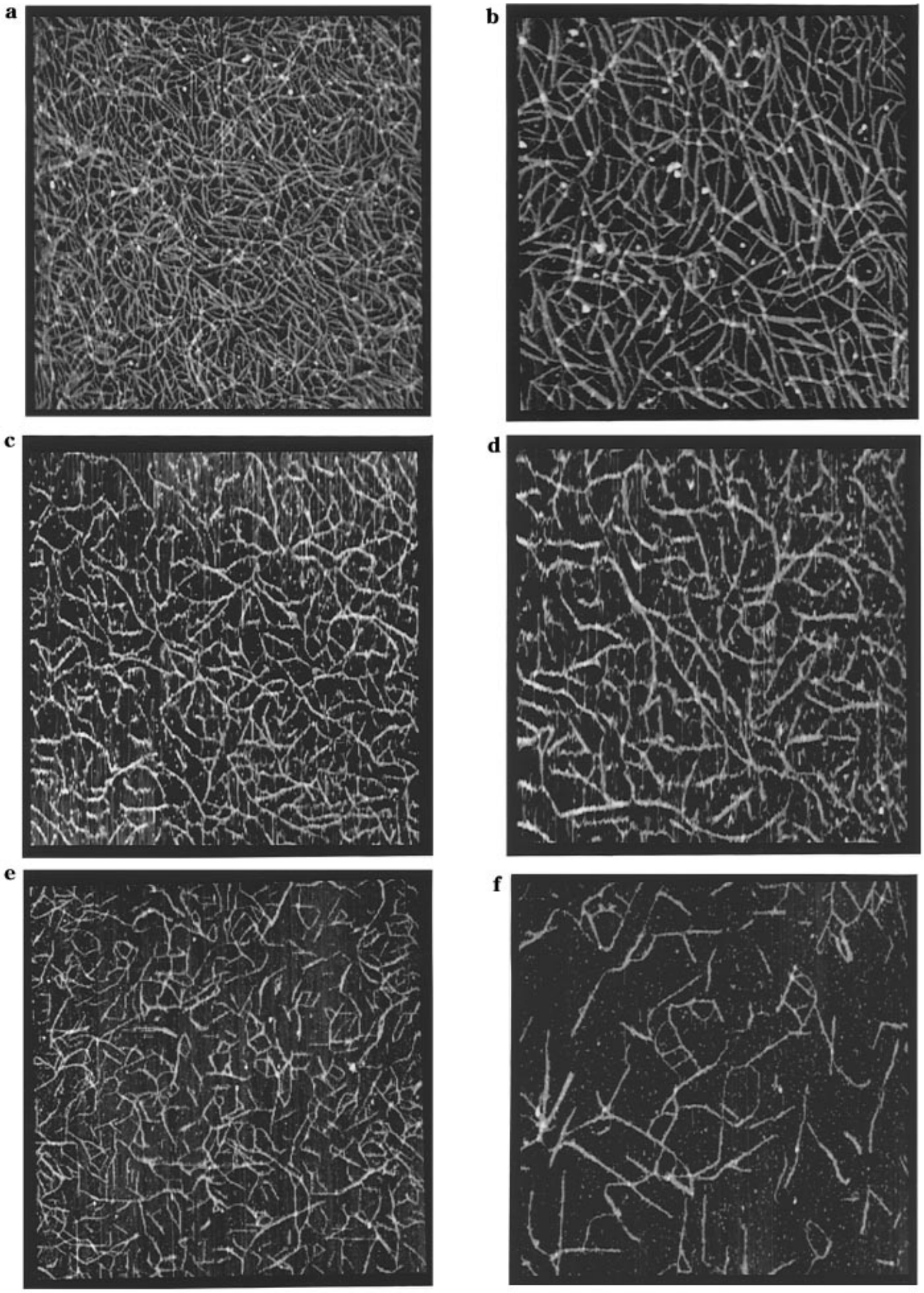

Figure 1. Gellan gum networks and aggregates. Deposition from 10 μg mL^{-1} K$^+$ gellan onto mica: (a) image size 1.6 × 1.6 μm and (b) image size 800 × 800 nm. Deposition from 10 μg mL^{-1} TMA gellan onto mica: (c) image size 1.5 × 1.5 μm and (d) image size 700 × 700 nm. Deposition from 3 μg mL^{-1} K$^+$ gellan onto mica: (e) image size 1.6 × 1.6 μm and (f) image size 800 × 800 nm.

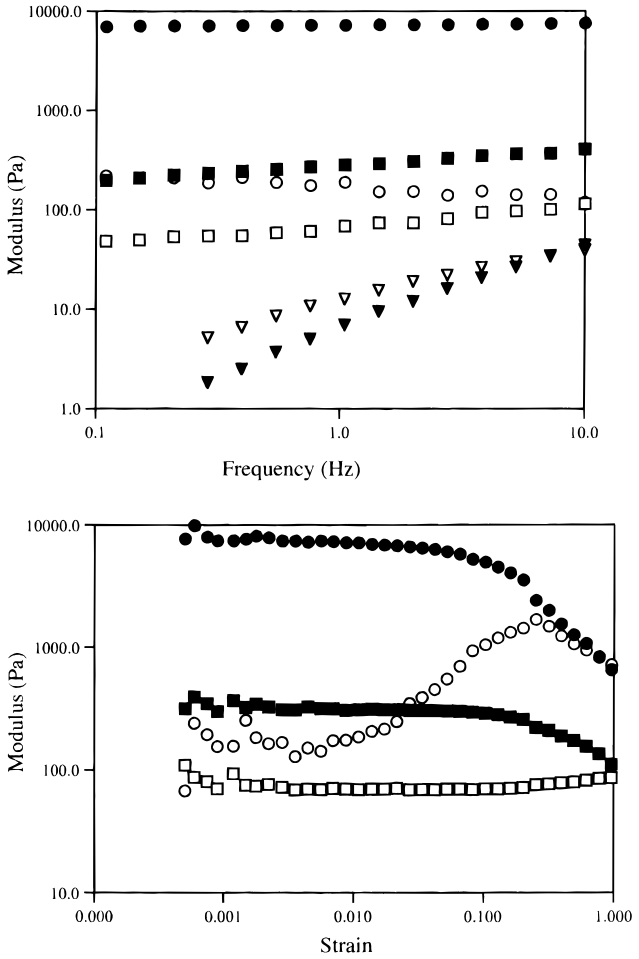

Figure 2. Rheology of gellan samples. (a) Frequency dependence of the moduli: G' (●) and G''(○) for 1.2% acid-set gellan gel, G′ (■) and G″ (□) for 1.2% K^+ gellan gel, and G' (▼) and G'' (▽) for 1.2% TMA gellan sample. Data recorded at a strain of 5%. (b) Strain dependence of K^+ and acid-set gels. Filled symbols, G'; open symbols, G″. □, K^+ gels; ○, acid-set gels.

structures representative of the structures formed in bulk aqueous gels? Also, it would be difficult to use 2D networks to study the effects of pH or ionic strength. On air-drying, crystallization of salts present would obscure or disrupt the network. Ideally it would be preferable to image the molecular structure of the bulk gel directly. At present there are only a few publications on AFM of films and gels[4,7,14−17] and no studies on polysaccharide gels. Studies on gelatin films have failed to achieve molecular resolution.[14,17] Radmacher and co-workers[14] have imaged gelatin films under various liquids. Using a series of water−alcohol mixtures to increase the Youngs' modulus of the film/gel, they obtained images with improved resolution.[14]

A 1.2% K^+ gellan gel was produced on mica and imaged under butanol after setting. Very poor images were obtained and imaging conditions were unstable. As shown in Figure 2, the shear modulus for these gels is low (∼350 Pa). Thus the poor resolution probably results from deformation of the gel surface during imaging. In order to reduce this effect, and following the conclusions of Radmacher and co-workers,[14] the shear modulus of the gels was increased. This was carried out in the following manner. A 1.5% K^+ gellan gel was melted and a freshly prepared solution of D-gluconic acid lactone (also known as glucono-δ-lactone GDL) was added to a final concentration of 0.3%. The gel was then thermally set on the mica surface. Addition of GDL lowered the gellan concentration to 1.2%. Hydrolysis of GDL reduces the pH and the acid-set gel forms when the pH is below the pK_a of charge groups on the gellan molecule. Acid-set gellan gels are known to yield the highest modulus values.[36] Figure 2 shows that the modulus has increased to $\sim 10^4$ Pa. It proved possible to image the surface of these gels under butanol (Figures 3 and 4).

Imaging was carried out under butanol in order to compare images of networks and gels. Immersion of bulk gellan gels in butanol results in some shrinkage. No significant changes in volume were observed over the period of time for which imaging was carried out. However, during the time scale for AFM imaging, some shrinkage probably occurs at the surface of the gel. Indeed imaging conditions were unstable for about 0.5 h after immersing the mica containing the gel into the butanol. Once the system has stabilized we have found that reproducible images can be obtained of gel surfaces. Representative images of a typical gel are shown in Figure 3a−d. At the highest scan sizes (Figure 3a) the image shows a homogeneous fibrous network similar to that observed for the 2D networks or films. The image contains regions which appear dark and others which are bright or flared. This effect arises due to the curvature or roughness of the gel surface. The number of gray levels required to define the molecular structure over the whole image cannot all be perceived by the eye. Thus, in the extreme peaks and troughs, molecular information cannot be perceived even though the information is actually present within the image. A number of techniques can be used to improve these topographical images. High pass filtering can be used to emphasize molecular (high frequency) information. Local smoothing can be used to average out high frequency (molecular) detail revealing the low frequency surface curvature which can then be subtracted from the original image to produce an artificially flattened image. The simplest approach is perhaps to collect data over smaller scan sizes (Figures 3b−d) and if necessary prepare a montage of such images.

Other experimental alternatives are shown in Figure 4. Rather than collecting a set of images and preparing a montage, it may be preferable to collect a single large image and zoom into particular regions of the image. This can be achieved by imaging at a very high pixel density. Figures 1a−f and 3a−d are images containing 256 × 256 pixels. Figure 4 shows an image collected using 1024 × 1024 pixels. Thus Figure 4 could be zoomed in order to produce an array of 16 images with a pixel resolution equivalent to Figures 1 or 3.

The images shown in Figures 3 and 4 indicate that the surface of a 3D gel resembles that of a 2D network. The gel structure consists of a gigantic branched fiber forming a 3D network. The gel contains 98.8% water. Some dehydration may occur at the gel−air surface after preparation, and further dehydration may occur after immersion under butanol. Hence the fiber density may be higher at the surface than in the bulk of the gel.

The fibrous nature of the gellan gel network is also consistent with other studies on gellan gels. Light-scattering studies of gellan gels suggest an average mass per unit length of ∼19 000 Da nm^{-1}, implying side-by-side aggregation of a few (two or three) gellan helices.[37] Similarly, small angle X-ray scattering studies are also consistent with side-by-side association of a few (ca. six) gellan helices.[26,27] Such models are compatible with the high transparency of the bulk gels and with fibrous branched structures reported for pregelling gellan samples studied by electron microscopy.[38]

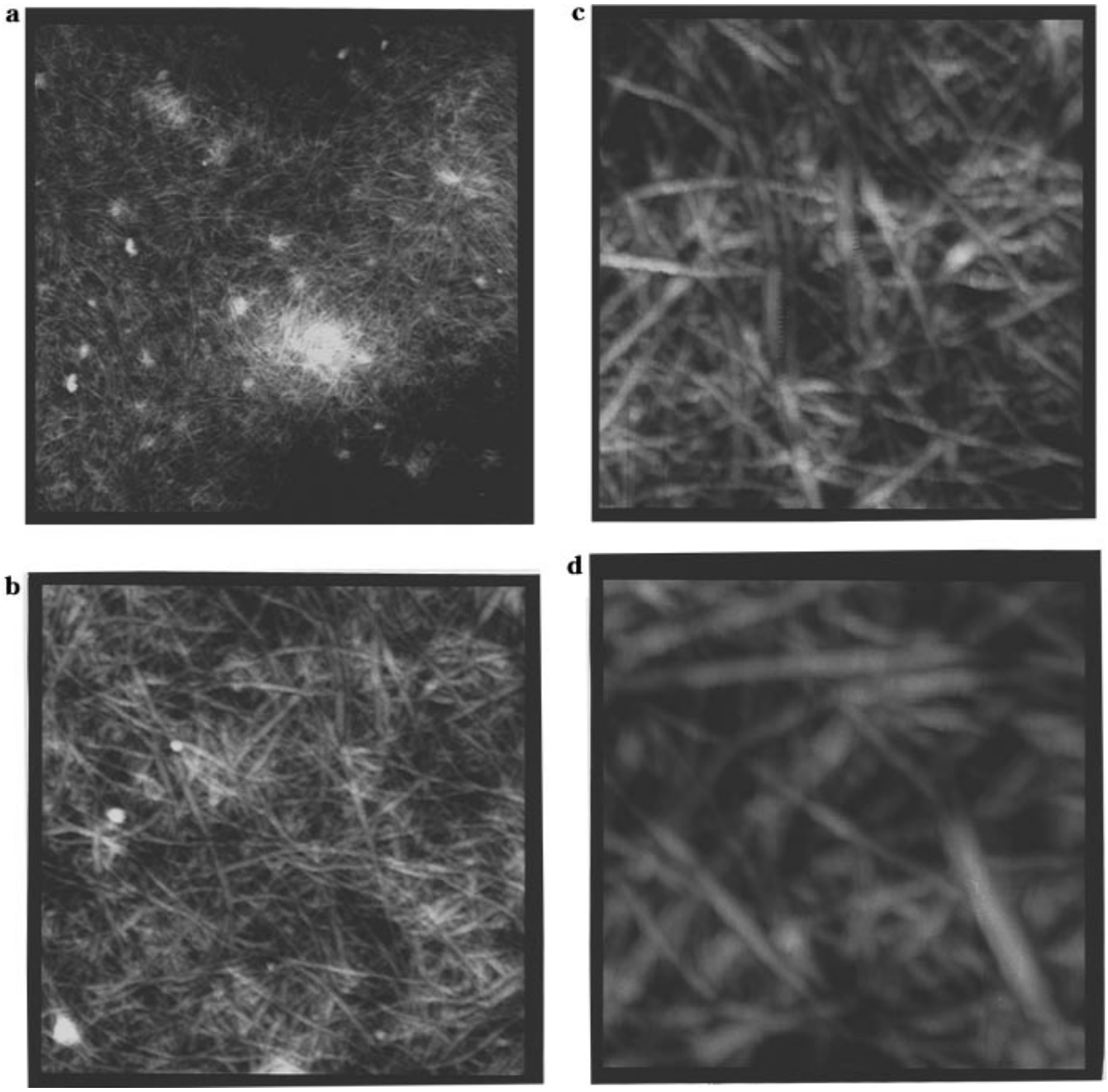

Figure 3. AFM images of bulk aqueous acid-set 1.2% gellan gel. Pixel density 256 × 256. Image sizes: (a) 5 × 5 μm, (b) 2 × 2 μm, (c) 1 × 1 μm, and (d) 500 × 500 nm.

The images presented in this paper are consistent with the following observations. The conformational change from coil to helix results in assembly of gellan molecules into elongated and/or branched aggregates. Above the critical or threshold concentration for gelation, these gel precursors are themselves assembled into a single fibrous network in the presence of gel-promoting cations. The permanency of the gel network arises due to ion binding between gellan helices stacked side-by-side within the fibers. Such a model for gellan gelation has been suggested[24,39] on the basis of light-scattering data.[39] The cation binding is considered to cause the observed hysteresis in melting and setting of gellan gels.[24,25] In the case of the 1.2% acid-set gellan gel used in the present study, this hysteresis is sufficient to make the gel thermally irreversible.

This type of fibrous model for gellan gels differs from the conventional model for polysaccharide gels. Polysaccharide gels are normally considered[40] to consist of junction zones formed by association of ordered helical regions linked by essentially disordered sections of the polysaccharide chain. In the images shown in Figures 1, 3, and 4 the entire fibrous structure is effectively a junction zone.

Conclusions

The present studies on gellan gum indicate that AFM can be used to probe polysaccharide association important for the gelation of polysaccharides. 2D networks or films can be prepared by air-drying suitably high concentration gellan sols after deposition onto mica surfaces. At nongelling concentrations, or after manipulation of counterions, it is possible to image gellan aggregates or gel precursors. Such model systems provide a means of investigating mechanisms of gelation. Preliminary studies have revealed that under favorable conditions it is possible to image the molecular architecture at the surface of 3D bulk aqueous gels. The images obtained have provided new insights into mechanisms for gellan gum gelation favoring a fibrous rather

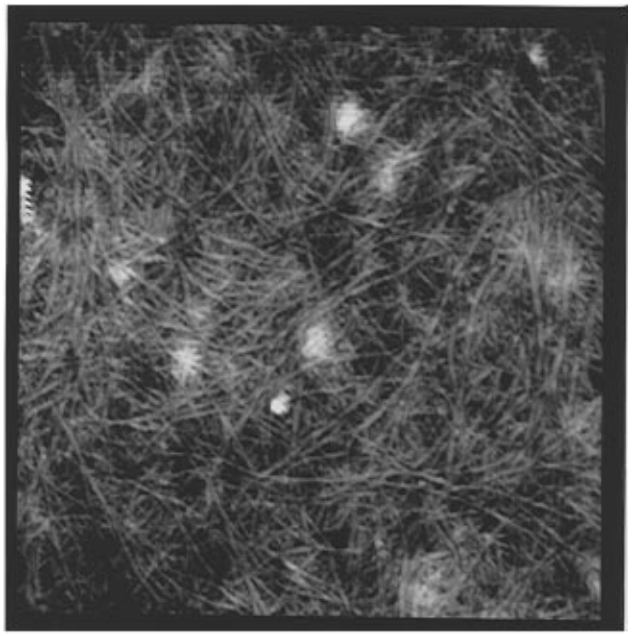

Figure 4. High pixel density (1024 × 1024) image of a bulk aqueous acid-set 1.2% gellan gel. Image size 3 × 3 μm.

than micellar model. Since gellan gum is often considered a model system for polysaccharide gelation, it is possible that the structures of other polysaccharide gels are similar in nature.

Acknowledgment. All authors acknowledge support for the present research from BBSRC.

References and Notes

(1) Engel, A. *Annu. Rev. Biophys. Biophys. Chem.* **1991**, *20*, 79.
(2) Hansma, H. G.; Hoh, J. H. *Annu. Rev. Biophys. Biomol. Struct.* **1994**, *23*, 115.
(3) Morris, V. J. *Prog. Biophys. Mol. Biol.* **1994**, *61*, 131.
(4) Gunning, A. P.; Kirby, A. R.; Morris, V. J.; Wells, B.; Brooker, B. E. *Polym. Bull.* **1995**, *34*, 615.
(5) Kirby, A. R.; Gunning, A. P.; Morris, V. J. *Carbohydr. Res.* **1995,** *267*, 161.
(6) Kirby, A. R.; Gunning, A. P.; Morris, V. J.; Ridout, M. J. *Biophys. J.* **1995**, *68*, 360.
(7) Kirby, A. R.; Gunning, A. P.; Morris, V. J. *Biopolymers* **1996**, *38*, 355.
(8) McIntire, T.; Penner, R. M.; Brant, D. A. *Macromolecules* **1995**, *28*, 6375.
(9) Guckenberger, R.; Heim, M.; Cevc, G.; Knapp, H. F.; Wiegräbe, W.; Hillebrand, A. *Science* **1994**, *266*, 1538.
(10) Martin, L. D.; Vesenka, J. P.; Henderson, E.; Dobbs, D. L. *Biochemistry* **1995**, *34*, 4610.
(11) Dammer, U.; Popescu, O.; Wagner, P.; Anselmetti, D.; Güntherodt, H-J.; Misevic, G. N. *Science* **1995**, *267*, 1173.
(12) Zhong, Q.; Inniss, D.; Kjoller, K.; Elings, V. B. *Surf. Sci-Lett.* **1993**, *290*, L688.
(13) Gunning, A. P.; Kirby, A. R.; Morris, V. J. *Ultramicroscopy*, in press.
(14) Radmacher, M.; Fritz, M.; Hansma, P. K. *Biophys. J.* **1995**, *69*, 264.
(15) Suzuki, A.; Yamazaki, M.; Kobiki, Y. *J. Chem. Phys.* **1996**, *104*, 1751.
(16) Wigren, R.; Billsten P.; Erlandsson, R.; Löfås, S.; Lundström, I. *J. Colloid Int. Sci.* **1995**, *174*, 521.
(17) Haugstad, G.; Gladfelter, W. L.; Keyes, M. P.; Weberg, E. B. *Langmuir* **1993**, *9*, 1594.
(18) Wong, T. M. H. PhD thesis, University of Cambridge, UK, 1991.
(19) O'Neil, M. A.; Selvendran, R. R.; Morris, V. J. *Carbohydr. Res.* **1983**, *124*, 123.
(20) Jansson, P-E.; Lindberg, B.; Sandford, P. A. *Carbohydr. Res.* **1983**, *124*, 135.
(21) Kuo, M. S.; Mort, A. J.; Dell, A. *Carbohydr. Res.* **1986**, *156*, 173.
(22) Sandford, P. A.; Cottrell, I. W.; Pettitt, D. J. *Pure Appl. Chem.* **1984**, *56*, 879.
(23) Baird, J. K.; Sandford, P. A.; Cottrell, I. W. *Bio. Technol.* **1983**, *1*, 778.
(24) Morris, V. J. *Food Polysaccharides and their Applications;* Stephen, A. M., Ed; Marcel Dekker: New York, 1995; Chapter 11, p 341.
(25) Robinson, G.; Manning, C. E.; Morris, E. R.; *Food Polymers, Gels and Colloids*; Dickinson, E., Ed; Royal Society Chemistry: London, 1991; p *22*.
(26) Yugichi, Y.; Mimura, M.; Kitamura, S.; Urakawra, H.; Kajiwara, K. *Food Hydrocolloids* **1993**, *7*, 373.
(27) Yoshide, H.; Takahashi, M. *Food Hydrocolloids* **1993**, *7*, 387.
(28) Carroll, V.; Miles, M. J.; Morris, V. J.; *Int.J. Biol. Macromol.* **1982**, *4*, 432.
(29) Attwool, P. T.; Atkins, E. D. T.; Upstill, C.; Miles, M. J.; Morris, V. J.; *Gums and Stabilisers for the Food Industry. 3*; Phillips, G. O., Wedlock, D. J., Williams, P. A., Ed.; IRL Press: Oxford, 1986; p 135.
(30) Chandrasekaran, R.; Millane, R. P.; Arnott, S.; *Gums and Stabilisers for the Food Industry. 4*; Phillips, G. O., Wedlock, D. J., Williams, P. A., Ed.; IRL Press: Oxford, 1988; p 183.
(31) Chandrasekaran, R.; Puigjaner, L. C.; Joyce, K. L.; Arnott, S. *Carbohydr. Res.* **1988**, *181*, 23.
(32) Chandrasekaran, R.; Millane, R. P.; Arnott, S.; Atkins, E. D. T. *Carbohydr. Res.* **1988**, *175*, 1.
(33) Chandrasekaran, R.; Radha, A.; Thailambal, V. G. *Carbohydr. Res.* **1992**, *224*, 1.
(34) Chandrasekaran, R.; Thailambal, V. G. *Carbohydr. Res.* **1990**, *12*, 431.
(35) Dentini, M.; Coviello, T.; Burchard, W.; Crescenzi, V. *Macromolecules* **1988**, *21*, 3312.
(36) Grasdalen, H.; Smidsrød, O. *Carbohydr. Polym.* **1987**, *7*, 371.
(37) Burne, P. M.; Sellon, D. B. *Biopolymers* **1994**, *34*, 371.
(38) Stokke, B. T.; Elgsaeter, A.; Kitamura, S. *Int. J. Biol. Macromol.* **1993**, *15*, 63.
(39) Gunning, A. P.; Morris, V. J. *Int.J. Biol. Macromol.* **1990**, *12*, 338.
(40) Rees, D. A.; Morris, E. R.; Thom, D.; Madden, J. *The Polysaccharides*; Aspinall, G. O., Ed.; Academic Press: New York, 1982; Vol. 1, p 195.

MA960700H